

Dalton Transactions

Accepted Manuscript

Downloaded by University of York on 02 July 2012
Published on 28 June 2012 on http://pubs.rsc.org | doi:10.1039/C2DT13114G



This is an *Accepted Manuscript*, which has been through the RSC Publishing peer review process and has been accepted for publication.

Accepted Manuscripts are published online shortly after acceptance, which is prior to technical editing, formatting and proof reading. This free service from RSC Publishing allows authors to make their results available to the community, in citable form, before publication of the edited article. This *Accepted Manuscript* will be replaced by the edited and formatted *Advance Article* as soon as this is available.

To cite this manuscript please use its permanent Digital Object Identifier (DOI®), which is identical for all formats of publication.

More information about *Accepted Manuscripts* can be found in the [Information for Authors](#).

Please note that technical editing may introduce minor changes to the text and/or graphics contained in the manuscript submitted by the author(s) which may alter content, and that the standard [Terms & Conditions](#) and the [ethical guidelines](#) that apply to the journal are still applicable. In no event shall the RSC be held responsible for any errors or omissions in these *Accepted Manuscript* manuscripts or any consequences arising from the use of any information contained in them.

Novel Pd(II)-Salen complexes showing high *in vitro* anti-proliferative effects against human hepatoma cancer by modulating specific regulatory genes

Mohammad Azam^{1*}, Zahid Hussain², Ismail Warad¹, Saud I. Al-Resayes¹, Mohd. Shahnawaz Khan³, Mohammad Shakir⁴, Agata Trzęsowska-Kruszynska⁵ and Rafal Kruszynski⁵

¹*Department of Chemistry, King Saud University, P. O. Box 2455, Riyadh 11451, KSA*

²*Center of Excellence in Biotechnology Research, King Saud University, Riyadh, 11451, KSA*

³*PRC, Department of Biochemistry, King Saud University, Riyadh 11451, KSA*

⁴*Department of Chemistry, Aligarh Muslim University, Aligarh 202002 India*

⁵*Department of X-ray Crystallography and Crystal Chemistry, Institute of General and Ecological Chemistry, Technical University of Lodz, Zeromskiego 116, 90-924, Lodz, Poland*

Author for Correspondence:

Mohammad Azam

Email: azam_res@yahoo.com Tel: +966-596441517

Abstract:

We have reported the synthesis of a novel Salen ligand and its mononuclear Pd-Salen complexes derived from 2-[2-hydroxy-3-[(E)-(2-hydroxyphenyl)methylidene]amino]propyl)imino]methyl}phenol. The newly synthesized and isolated Pd(II) complexes have been identified and fully characterized by various physico-chemical studies viz., elemental analyses, IR, UV-Vis, ^1H , ^{13}C NMR spectroscopy, Electron Spray Ionization Mass Spectrometry (ESI-MS) and TGA/DTA studies. The molecular structure of salen ligand has been ascertained by single crystal XRD and it is coordinated to Pd(II) ion through two nitrogen and two oxygen atoms. The UV-Vis data clearly suggest a square planar environment around both the Pd(II) ions. The DNA binding studies of the synthesized compounds has been investigated by electron spectroscopy and fluorescence measurements. The results suggest that Pd(II) complexes bind to DNA strongly as compared to free ligand. The free salen ligand and its Pd(II) complexes have also been tested against human hepatoma cancer cell line (Huh7) and results manifested exceptional anti-proliferative effects of Pd(II) complexes. The anti-proliferative activity of Pd(II) complexes has been modulated by specific regulatory genes.

Keyword: Salen ligand, Pd(II) complexes, Physico-chemical studies, DNA binding, anti-proliferative, human hepatoma cell, gene expression

1. Introduction:

Since the revolutionary discovery of cisplatin, chemically named as *cis*-(diamminedichloroplatinum(II)) as an anticancer drug by Rosenberg, extensive research work has been carried out on platinum based chemotherapeutic compounds [1-2]. Despite its remarkable success with high efficacy against human testicular, ovarian, bladder, head and neck carcinomas, several side effects such as limited water solubility and the dose-dependent toxicities, mainly nephrotoxicity, neurotoxicity, cytotoxicity, and emetogenesis are the major drawbacks associated with this drug [3-5]. Besides this, prolonged use of cisplatin also leads to cellular resistance in some of the most common cancers [6]. Therefore, to overcome these problems, attempts are being made to replace this drug with suitable alternatives, and numerous transition-metal complexes have been synthesized and screened for their anticancer activities [6]. The first non-platinum complex tested in clinical trials was *cis*-[(CH₃CH₂O)₂(bzac)₂Ti(IV)] used against a wide variety of ascites and solid tumors [7-8]. The significant similarity between the coordination chemistry of Pd(II) and Pt(II) compounds has advocated studies of Pd(II) complexes as antitumor drugs, but the higher lability in ligand exchange at Pd centre (10⁵-fold vs Pt) may cause rapid hydrolysis processes leading to dissociation of complex and formation of very reactive species unable to reach their pharmacological targets [9]. These problems could be overcome by using the bulky heterocyclic and chelating ligands. A number of palladium complexes with aromatic N- and N,N-containing ligands have shown very promising antitumor characteristics [10,11]. Recent studies demonstrate that some Pd(II) complexes exhibit a noticeable *in vitro* cytotoxic activity, comparable to standard platinum-based drugs, cisplatin, carboplatin and oxaliplatin [12]. Over the years chemists have prepared ligands with a wide range of features designed to achieve their particular targets. In this context, the chemistry of

[View Online](#)

metal complexes containing salen-type ligands has received a lot of attention because of their versatility and wide range of complexing ability, and are also the key points in the development of inorganic biochemistry, catalysis, magnetism, medical imaging etc. [13-16]. Some of the salen complexes have also revealed interesting antioxidant and antitumor properties [17]. Here in this article, we report the synthesis and characterization of a novel salen ligand derived from 1,3-diaminopropanol and o-hydroxybenzaldehyde and its Pd(II) complexes. The synthesized ligand and its complexes have been screened for their *in vitro* viability and anti-proliferative activities in human hepatocellular carcinoma (Huh7) cells. We have also analyzed the effect of salen ligand and its Pd(II) complexes on the expression of the key genes involved in tumor promoting and tumor suppressing function; such as Wnt-1, Urokinase plasminogen activator (uPA), Ras association domain family 1A (RASSF1A), and transforming growth factor- β (TGF- β).

2. Experimental:

2.1 Materials and Methods

All the reagents and solvents used were of analAR grade quality and were purchased from Merck and used as received. All complexations reactions were carried out using standard schlenk techniques under argon. Elemental analyses were recorded on Elementar Vario EL analyzer. FT-IR (4000–400 cm^{-1}) spectra were obtained as a KBr pellet using Perkin Elmer 621 spectrophotometer. ^1H and ^{13}C NMR spectra of ligand and its Pd(II) complexes were recorded in CDCl_3 using JEOL 400 spectrometer. Chemical shifts are quoted in parts per million from TMS. Mass spectrometry was performed with a Micromass Quattro Premier tandem MS fitted with an ESI interface and controlled by MassLynx 4.1 software. MS/MS detection was performed with electrospray positive ionization mode. Electronic spectra of the complexes were obtained in dichloromethane on Pharmacia LKB-Biochem, UV-vis spectrophotometer at room temperature.

Thermal behavior of the synthesized compounds was studied by using SDTQ-600 (TA Instrument) in helium atmosphere (100 mLmin^{-1}) at heating rate of $20 \text{ }^\circ\text{C/min.}$, in the temperature range from ambient to $800 \text{ }^\circ\text{C}$.

2.2 Synthesis:

2.2.1 Synthesis of salen ligand: *L*

A methanolic solution of *o*-hydroxybenzaldehyde (2 mmol) was added dropwise to the methanolic solution of 1,3-diaminopropanol (1 mmol). The reaction mixture was stirred for 5 h resulting in to a clear yellow colored solution. The resulting colored solution was concentrated to 1 ml followed by addition of 20 ml of diethyl ether to cause precipitation. Precipitate was removed by filtration. After couple of days, yellow crystals suitable for X-ray diffraction appeared in filtrate. The crystals were filtered off, washed with hexane and dried in vacuo.

Yield 70 %, Color: Yellow, Mp.: $138 \text{ }^\circ\text{C}$; Molecular formula $\text{C}_{17}\text{H}_{18}\text{N}_2\text{O}_3$; $^1\text{H NMR}$ (CDCl_3): δ (ppm) 13.82 (Ar-OH), 8.35 (s -CH=N), 6.79-7.10 (m, Ar-H), 3.58-3.65 (m 4H -CH₂), 3.65 (s, 1H, -CH). $^{13}\text{C NMR}$ (CDCl_3): δ (ppm) 163.68 (-CH=N), 62.85 (-CH₂), 69.15 (-CH), 160.15, 131.85, 131.91, 116.45, 118.50 and 117.21 (Aromatic carbons), *Anal. Cal:* C, 68.44; H, 6.08; N, 9.39; O, 16.08 % *Found:* C, 68.25; H, 5.97; N, 9.28; O, 15.98 % IR, 3270 cm^{-1} ($\nu_{\text{Ph-OH}}$), 1655 cm^{-1} ($\nu_{\text{-CH=N}}$), 1278 cm^{-1} ($\nu_{\text{Phenolic C-O}}$).

2.2.2 Synthesis of Complexes: $[\text{PdLCl}_2]$ **1** and $[\text{PdL}(\text{OAc})_2]$ **2**

A solution of Pd(II) salt (0.50 mmol) dissolved in 10 ml CH_2Cl_2 was added dropwise in 10 ml CH_2Cl_2 solution of ligand (0.50 mmol). The resultant reaction mixture was stirred for half an hour resulting in to a clear yellow colored solution. The resulting solution was concentrated to 1 ml followed by addition of 10 ml of hexane for precipitation. The resulting colored precipitate

was isolated and recrystallised in dichloromethane-hexane mixture and obtained in analytically pure form. No crystal was found suitable for single crystal XRD.

1 : Yield 70 %, Color: Yellow, Mp.: 138 °C; Molecular formula $C_{17}H_{18}N_2O_3PdCl_2$; 1H NMR ($CDCl_3$): δ (ppm) 8.41 (s -CH=N), 6.89-6.97 (m, Ar-H), 3.87 (s, 1H, -CH), 3.86-3.72 (m 4H -CH₂). ^{13}C NMR ($CDCl_3$): δ (ppm) 167.56 (-CH=N), 63.36 (-CH₂), 70.58 (-CH), 161.03, 132.71, 131.68, 118.92, 118.72 and 117.07 (Aromatic carbons), *Anal. Cal*: C, 42.93; H, 3.81; N, 5.89; O, 10.09; Pd, 22.37; Cl, 14.91 % Found: C, 42.88; H, 3.79; N, 5.85; O, 9.98; Pd, 22.32; Cl, 14.85 % IR, 1290 cm^{-1} (ν_{Pd-O}), 1625 cm^{-1} ($\nu_{CH=N}$)

2: Yield 70 %, Color: Yellow, Mp.: 138 °C; Molecular formula $C_{21}H_{24}N_2O_7Pd$; 1H NMR ($CDCl_3$): δ (ppm) 8.56 (s -CH=N), 6.87-7.97 (m, Ar-H), 5.23 (s, 1H, -CH), 3.61-3.75 (m 4H -CH₂), ^{13}C NMR ($CDCl_3$): δ (ppm) 172.25 (-CH=N), 63.85 (-CH₂), 70.15 (-CH), 167.85, 161.80, 132.15, 132.25, 117.75, 118.23 (Aromatic carbons), *Anal. Cal*: C, 48.24; H, 4.62; N, 5.35; O, 21.42; Pd, 20.35 % Found: C, 48.19; H, 4.57; N, 5.31; O, 21.37; Pd, 20.28 % IR, 1282 cm^{-1} (ν_{Pd-O}), 1648 cm^{-1} ($\nu_{CH=N}$)

2.3 Crystal structure determination

The yellow prism crystal of free **L** was sealed in glass capillary filled with helium and next it was mounted on a KM-4-CCD automatic diffractometer equipped with CCD detector, and used for data collection. X-ray intensity data were collected with graphite monochromated CuK_{α} ($\lambda = 1.54178 \text{ \AA}$) radiation at temperature 291.0(3) K, with ω scan mode. The 34 seconds exposure time was used, and reflections inside Ewald sphere were collected up to $\theta = 68.04^\circ$. The unit cell parameters were determined from 3008 strongest reflections. Details concerning crystal data and refinement are given in Table 1. Examination of reflections on two reference frames monitored after each 20 frames measured showed no loss of the intensity during measurement. During the

data reduction Lorentz, polarization and numerical absorption corrections were applied [18]. The structure was solved by partial structure expansion procedure. All the non-hydrogen atoms were refined anisotropically using full-matrix, least-squares technique on F^2 . All the hydrogen atoms were found from difference Fourier synthesis after four cycles of anisotropic refinement, and refined as “riding” on the adjacent atom with geometric idealisation after each cycle of refinement and individual isotropic displacement factors equal 1.2 times the value of equivalent displacement factor of the parent carbon atoms and 1.5 times of parent oxygen atoms. The hydroxyl groups were allowed to rotate about the O-C bond axes. The studied crystal was racemically twinned with the 0.56:0.44 participation of chiral domains. The Flack parameter was refined as full matrix parameter. The SHELXS97, SHELXL97 and SHELXTL programs were used for all the calculations [19]. Atomic scattering factors were those incorporated in the computer programs. Selected interatomic bond distances and angles are listed in Table 2 and intermolecular interactions are listed in Table 3.

2.4 DNA binding assays of free L and Complexes 1 and 2

DNA binding experiments were performed on UV-Vis and fluorescence spectroscopy. The purity of calf thymus DNA was confirmed by taking the ratio of the absorbance values at 260 and 280 nm in Tris EDTA (10mM, pH 7.0) buffer, which was found to be 1.8:1, indicating that the DNA was sufficiently free of protein and other contaminants. The concentration of DNA for binding studies was determined by absorption spectroscopy at 260 nm using the molar extinction coefficient value of $6600 \text{ dm}^3 \text{ mol}^{-1} \text{ cm}^{-1}$. The novel free **L** and its complexes **1** and **2** were dissolved in 5% DMSO. Absorption titration experiments were performed with a fixed

concentration of DNA (0.1mM) while gradually increasing concentration of free **L** and its complexes **1** and **2** from 10-50 μM .

Further, to strengthen the Ligand-DNA binding interaction, fluorescence quenching experiments were performed. Nucleic acid binding assays of synthesized compounds were carried out in the presence of ethidium bromide. DNA and ethidium bromide (EB) were dissolved in tris-EDTA (10 mM, pH 7.0) buffer at the concentrations of 4 and 1 $\mu\text{g/ml}$, respectively. The concentration of ligand, **L** and complexes **1** and **2** was 50 μM . To perform the experiments, DNA was pretreated with ethidium bromide for 30 min. Then the test solutions were added to this mixture of EB-DNA, and the change in the fluorescence intensity was measured. Fluorescence measurements were carried out on a Shimadzu spectrofluorimeter model RF-540 equipped with a data recorder DR-3. The fluorescence was recorded at 485–685 nm after exciting the solution at 478 nm. The slits were set at 5 nm for excitation and emission. The path length of the sample was 1 cm.

To determine the DNA-binding ability of free **L** and complexes **1** and **2**, fluorescence intensity data were analyzed by the Stern-Volmer equation [20].

$$F_0/F = 1 + K_{sv} [Q]$$

Where, F and F_0 are the fluorescence intensity with and without the quencher (complex-DNA), K_{sv} the Stern-Volmer quenching constant, and Q the concentration of the quencher. The K_{sv} value of the complexes [EB+DNA+**L**], [EB+DNA + **1**] and [EB+DNA+ **2**] were calculated to be 1.23×10^5 , 3.85×10^5 and $3.67 \times 10^5 \text{ M}^{-1}$, respectively. A higher K_{sv} value of complex **1** suggests its stronger quenching ability than complex **2** and free **L**.

2.5 Cell Culture and Treatment

Human hepatoma cell line Huh7, was grown in Dulbecco's modified Eagle's medium (DMEM, Gibco-BRL) supplemented with 10% fetal bovine serum (FBS, Gibco-BRL) and 10 μg of gentamycin ml^{-1} at 37°C in 5% CO_2 . In the treatment group, Huh7 cells treated for 48 hours with different test compounds (free **L**, Complexes **1** and **2** at final concentration of 0.1 μM , along with vehicle control alone (DMSO).

2.6 Cell Proliferation Assay

Huh7 cells were plated in quadruplicate at a density of 60,000 cells/well in 2 ml of respective culture media in six well plates. Cells were grown in the regular medium with 5% FBS in the control and treatment (free **L**, Complexes **1** and **2**) groups. Cell growth curve was analyzed at dose of (0.1 μM). Cells were trypsinized, and the number of viable cells was determined by 0.4% trypan blue and counted at different time points starting from day 0 to 48 hours, using a Coulter Counter (Model ZF; Coulter Electronics, Hertfordshire, UK).

2.7 Quantitative real time RT-PCR of genes involved in cancer

Total cellular RNA from control and treated (free **L**, Complexes **1** and **2**) Huh7 cells were extracted using Trizol (Invitrogen Life Technologies) according to manufacturer's protocol. Two micrograms of total RNA was used for reverse transcription for cDNA preparation. The cDNA was then used for quantitation of genes involved in cancer by real time PCR (Applied Biosystem, 7500 Real Time PCR system). The primers used to quantify different genes are mentioned in Table 4.

2.8 Statistical analysis

Results were analyzed as the mean \pm SEM, and comparisons of the experimental data were by two tailed independent sample student's *t*-test. *P* value of <0.05 was considered statistically significant.

3. Results and Discussions:

The free salen ligand, **L** has been synthesized by the interaction of *o*-hydroxybenzaldehyde with 1, 3-diaminopropanol in 2:1 molar ratio in methanolic medium (Scheme). Pd(II) complexes, synthesized by reaction of free **L** and Pd(II) salts in 1:1 molar ratio in dichloromethane in schlenk line under argon atmosphere, are colored microcrystalline solids. All the synthesized compounds are insoluble in water and soluble in all organic solvents. The formation of ligand and its Pd(II) complexes were confirmed on the basis of results of elemental analyses, molecular ion peak in ESI-MS spectra, characteristic absorption bands in FT-IR, and resonance signals in the ^1H and ^{13}C NMR spectra, and single crystal XRD in case of ligand. The geometry around Pd(II) ions in the complexes was confirmed from the positions of absorption bands observed in UV-Vis spectra. The *in vitro* cytotoxic activity of the isolated free **L** and its Pd(II) complexes have been tested against human Hepatoma Cancer Cell line, Huh7. Results suggest that Pd(II) complexes are more prominent in showing anti- proliferative activity when compared with parent salen ligand.

3.1 X-ray crystallography

A perspective view of free **L** shows that all atoms occupy the same general positions (Fig 1). The asymmetric part of the unit cell contains the four molecules of free **L**, and two of them (containing N41 and N61 atoms) are related by non-crystallographic pseudosymmetry centre. In general, the molecules possess different conformations (Table 2), however for the molecules

related by pseudosymmetry these differences are relatively small (Table 2). Some of the atoms of free **L** molecules show the differences in magnitude between components of the anisotropic displacement parameters along chemical bonds and in the equivalent isotropic displacement parameters in comparison to those ones of neighbouring bonded atoms. This originates primarily from twisted character of parts of studied molecules aliphatic chains (for details see torsion angles in Table 2) and thus more privileged motion and static disorder in directions perpendicular to the interatomic bonds. The 2-hydroxybenzylideneaminomethyl moieties of all molecules of free **L** are close to planarity, and however some obvious deviations of atoms from the respect weighted least squares planes exist, they are not larger than 0.04 Å. Mentioned moieties existing in duplicate within each molecule are inclined at 55.08(5), 62.15(5), 77.88(4) and 75.78(4)°, respectively for molecules containing N1, N21, N41, N61 atoms. The analysis of C-N bond lengths shows that the double bonds are fully localised within benzylideneamino moieties.

Each molecule of free **L** contains the two O—H•••N intramolecular hydrogen bonds within 2-hydroxybenzylideneamino moieties (Table 3), each forming S(6) motif. The molecules of **1** are connected by O—H•••O intermolecular interactions (Table 3) to hydrogen bonded tetramers, in which the hydroxyl substituents of molecule aliphatic part act as hydrogen bond donors, and hydroxyl substituents of aliphatic and aromatic parts act as hydrogen bond acceptors. The interactions form the N₁DDDD zero-dimensional unitary graph set, which is also zero-dimensional on higher graph set levels but it can be described as N₃C₃³(13) and N₄C₃³(13)D. In the structure can be found two intramolecular C—H•••N and one intermolecular C—H•••O short contacts (Table 3) which can be classified as weak hydrogen bonds [21]. This last interaction expands the tetramers to the hydrogen-bonded pillar extending along crystallographic [001] axis.

The stacking interactions are not observed within the crystal structure of free **L** (the shortest distance between centroids of close to parallelity aromatic rings is 4.8026).

3.2 IR discussion

The most important IR bands and their assignments are listed in the experimental section. When comparing the spectroscopic data of Pd(II) complexes with those of free ligand, marked changes may be noticed in the ligand bands arising from various modes of donor groups involved in bonding to palladium ions [Fig 2]. The IR spectrum of salen ligand exhibits a characteristic $\nu_{(\text{CH}=\text{N})}$ stretching band at 1655 cm^{-1} which is shifted to lower frequency and appears at 1630 cm^{-1} for **1** and 1648 cm^{-1} for **2** thus, indicating the coordination of azomethine nitrogen to Pd(II) ion [22-24], which is further confirmed by the appearance of a band at $425\text{-}430\text{ cm}^{-1}$ assigned to $\nu_{(\text{Pd}-\text{N})}$ vibration [25]. The stretching band observed at ca. 3270 cm^{-1} due to the $\nu_{(\text{Ph}-\text{OH})}$ group in the free ligand disappears in Pd(II) complexes due to deprotonation. A band which appeared at 1278 cm^{-1} (Phenolic C-O) in the free ligand has been shifted to higher frequency and appears at 1290 cm^{-1} and 1282 cm^{-1} in **1** and **2**, respectively, suggesting the coordination through the phenolic oxygen atom [24]. The absorption band corresponding to $-\text{OH}$ group of diaminopropanol remain unchanged in Pd(II) complexes concluding that the $-\text{OH}$ group of diaminopropanol doesn't take part in coordination [26]. The absorption band appeared at 295 cm^{-1} are assigned to $\nu_{(\text{Pd}-\text{Cl})}$ vibration in **1**, while the **2** shows two absorption bands at 1637 cm^{-1} and 1430 cm^{-1} , assignable to $\nu_{\text{a}}(\text{COO})$ and $\nu_{\text{s}}(\text{COO})$ stretching vibrations of the carboxylate group, respectively, indicating the monodentate coordination of the acetate group to Pd(II) ion [27].

3.3 ^1H and ^{13}C NMR Spectroscopic analyses

The ^1H NMR spectrum of the free ligand exhibits a singlet at 13.82 assigned to the aromatic-OH proton, which is absent in Pd(II) complexes indicating the coordination of phenolic oxygen to Pd(II) ion. A significant azomethine proton due to $-\text{CH}=\text{N}$ was observed at 8.35 ppm, which upon coordination to Pd(II) ion showed a downfield shift and occurred at 8.41 and 8.56 ppm for **1** and **2**, respectively [Fig 3] [Fig 1S supporting information]. ^1H NMR spectrum of ligand, **L** also shows a series of multiplets due to aromatic protons in the 6.79–7.10 ppm range. As expected, upon coordination to Pd(II) ion, these signals show small shifts due to the ligand electronic redistribution attributed due to interaction of ligand to Pd(II) ion. In addition, chemical shifts for $-\text{CH}$ (s 1H) and $-\text{CH}_2$ (d 4H) protons in free ligand appear at 3.65 ppm and 3.58–3.65 ppm, respectively. The findings of ^1H NMR spectra are further supported by ^{13}C NMR spectra [Fig 4] [Fig 2S]. The ^{13}C NMR spectrum of salen ligand shows a number of signals corresponding to various carbon atoms in the proposed ligand, expected due to the non-equivalence of the various carbon atoms. The free **L** shows sharp signal corresponding to azomethine carbon at 163.68 ppm while the signal for $-\text{CH}_2$, and $-\text{CH}$ carbon appears at 62.85 and 69.15 ppm, respectively. The ^{13}C NMR signals for aromatic carbon appear at 160.15, 131.85, 131.91, 116.45, 118.50 and 117.21 ppm. These values undergo downfield shift upon coordination to Pd(II) ion. The complex **2** shows a sharp signal at 172.25 ppm attributed to $-\text{CH}=\text{N}$ carbon while the signals for $-\text{CH}_2$, $-\text{CH}$ carbon appear at 63.85, 70.15 ppm. The signals for aromatic carbon appear at 160.75, 161.80, 132.15, 132.25, 117.75 and 118.23 ppm [Fig 4]. Similarly, sharp signal for azomethine carbon appears at 167.57 ppm in complex **1**. The signals for $-\text{CH}_2$ and $-\text{CH}$ carbon appear at 63.36 ppm and 70.58 ppm, respectively, while the signals for aromatic carbon appear at 161.03, 132.71, 131.68, 118.92, 118.72 and 117.07 [Fig 2S].

3.4 Mass spectrometry

The structure of the complexes was also supported by mass spectrometry under positive ion ESI condition. The ESI-MS spectra of the synthesized ligand and its Pd(II) complexes show the presence of the molecular ion as sodium adduct $[M+Na]^+$. The ESI-MS spectra showed molecular ion peaks $[M+Na]^+$, m/z at 299.34, 476.67, 522.84 corresponding to their molecular formulae, L, $[PdLCl_2]$ and $[PdL(OAc)_2]$, while their corresponding calculated m/z being 298.34, 475.67, 522.85, respectively [Fig 5].

3.5 UV-Vis studies

UV-Vis absorption spectra of Pd(II) complexes have been recorded in the 200–800 nm range in dichloromethane [Fig 6]. The bands below 321 nm are attributed to $\pi-\pi^*$ and $n-\pi^*$ transitions of the ligands [28,29]. All Pd(II) complexes are diamagnetic with a square-planar geometry, for which three spin-allowed d–d transitions are expected, corresponding to transitions from the three lower lying d-levels to the empty dx^2-y^2 orbitals [30]. The most prominent absorption bands appears at 401 nm and 397 nm for **1** and **2**, respectively, ascribed to the metal-to ligand charge transfer transitions [28, 29].

3.6 Thermogravimetric analyses

Thermal stabilities of **1** and **2** were carried out by thermogravimetric analyses (TGA and DTA) in N_2 atmosphere at heating rate of $20\text{ }^\circ\text{C min}^{-1}$ in the temperature range 20–800 $^\circ\text{C}$. These compounds undergo three steps of weight losses [Fig 7]. The TGA of **2** shows first weight loss of 11.45 % corresponding to coordinated water and acetate ion in the temperature range of 30–252 $^\circ\text{C}$. Further elevation in temperature from 252–485 $^\circ\text{C}$ leads to rapid weight loss ca. 48.55 % attributed to the dissociation of the salen ligand at the imine bond. A gradual weight loss in the temperature range 485–800 $^\circ\text{C}$ leads to the complete decomposition of organic moiety, until the

final residue, Pd-O, is left. Thus the total weight loss upto 800 °C is found to be 60 %. The TGA data is further supported by DTA, which shows three main steps at 20-200 °C, 200-452 °C and 452-800 °C. The maximum weight loss ca. 14 %/min occurred in the second stage at 200-452 °C. The result of TGA and DTA clearly indicated that the second stage is the main degradation stage.

3.7 DNA binding studies

UV–Vis absorption studies were performed to further ascertain the interaction of ligand and its Pd(II) complexes with DNA. The UV absorbance showed an increase in absorbance at 260 nm with increasing concentrations of free **L** and complexes **1** and **2** [Fig 8]. The rise in the DNA absorbance is indicative of the interaction between DNA and synthesized compounds. The obtained results showed that free **L** and its complexes exhibited hyperchromism (increase in absorbance) but of varied degree. Complexes **1** and **2** showed greater affinity for DNA as compared to free **L**. Interestingly, both the complexes, **1** and **2** showed approximately equal binding with DNA. Hypochromism and hyperchromism are both spectral features of DNA connected with its double helix structure. Hypochromism means the DNA-binding mode of the complex is electrostatic or intercalative which can stabilize the DNA duplex [31, 32]. Contrary to this hyperchromism means the breakage of the secondary structure of DNA. So we speculate that our synthesized compounds (free **L** and its Pd(II) complexes **1** and **2**) interact with the secondary structure of calf thymus DNA resulting in its breakage and perturbation.

Further, ethyidium bromide displacement assay for DNA binding study with free **L** and complexes **1** and **2** were executed using fluorescence spectroscopy. Nucleic acid bound to some molecules generally exhibit marked changes in fluorescence properties and this phenomenon is

[View Online](#)

used in the studies with DNA [33]. Ethidium bromide, a polycyclic aromatic dye, is the most widely used fluorescence probe for DNA structure. EB displays very weak fluorescence in aqueous solution. However, in the presence of DNA, it exhibits intense fluorescence because of the intercalation to base pairs in DNA [34]. Our results showed that the addition of free **L** and complexes **1** and **2** to DNA being complexed with EB causes appreciable reduction in emission intensity, indicating that synthesized compound have the ability of competitive binding with the EB for DNA and thus reaffirm the binding of these novel synthesized molecules with DNA. Moreover, results inflicted complexes **1** and **2** more quenching as compared to free **L**, thus indicating greater affinity of both the complexes when compared to ligand. On the basis of above mentioned results, we suggest that free **L** and complexes **1** and **2** have the ability to interact with DNA. However, the affinity for DNA is more in case of complexes **1** when compared with complex **2** and free **L**. The higher K_{SV} value implicates the higher binding affinity of complex **1** in comparison to complex **2** and free **L**. This difference in their DNA binding ability could be due to the presence of an electron deficient center in the charged Pd(II) complex where an additional interaction between the complex and phosphate rich DNA back bone may occur [35]. It has been reported that the enhanced fluorescence of the EB– DNA complex can be quenched at least partially by the addition of a second molecule and this could be used to assess the relative affinity of the molecule for DNA [Fig 9] [36].

3.8 Effect of free L, complexes 1 and 2 on cell proliferation

To test *in vitro* anti-proliferative effect of synthesized compounds (free **L**, complexes **1** and **2**) on hepatocellular carcinoma cell lines (Huh7), treatment dose was optimized to avoid cell cytotoxicity. Huh7 cells were seeded at the same density and subjected to optimum dose of these

compounds along with control (CTL) in six well plates. The optimized dose was used to treat at 0 hour and anti-proliferative effect was analyzed at different time 0, 12, 24 and 48 hours. As shown in Fig 1, number of cells at 12 hours of treatment was significantly less in complexes **1** and **2** treated wells. The effect of free **L** at 12 hours of treatment was similar to that of control. At 24 and 48 hours, the cells treated with complexes **1** and **2** showed significant anti-proliferative effects compared to free **L** and control (Fig 10 a and Fig 10 b) The complexes **1** and **2** significantly reduce the cell doubling time as well it showed limited cytotoxicity. Thus, our anti-proliferative data confirmed the role of complexes **1** and **2** in reducing the cell doubling time and hence proliferation.

3.9 Effect of free L, complexes 1 and 2 on tumor promoting genes

The cells treated with optimized concentration of free **L**, complexes **1** and **2** along with vehicle control alone were subjected to total cellular RNA isolation. The total cellular RNA was collected and analyzed for the expression of Wnt-1 and uPA mRNA levels. Our data indicate that Huh7 cells treated with complexes **1** and **2** significantly reduce the expression of Wnt-1 mRNA levels (Fig 11 a). The reduction was not significantly observed in alone treated Huh7 cells compared to control. Similar effects were not observed with the level of urokinase plasminogen activator (uPA) mRNA, when cells were treated with free **L**, complexes **1** and **2**. As shown in Fig 11b, uPA levels was almost similar to that of the vehicle control only. Our result demonstrated that complexes **1** and **2** reduce the tumor promoting gene Wnt-1 but not prometastatic gene uPA.

3.10. Effect of free **L**, **1** and **2** on tumor suppressor gene (*RASSF1A*)

Tumor suppressor gene (*RASSF1A*) has been studied in several cancers, and reported that large number of patients have inactivated *RASSF1*, while similar number have a tumor in which *RASSF1A* pathway is partially abrogated by inactivation of other signaling components. Since, it influences large number of proteins, the effect of compounds on the mRNA expression of *RASSF1A* have been investigated. Total cellular RNA (treated and control) was analyzed for the expression of *RASSF1A*. Our results show that complexes **1** and **2** treated Huh7 cells significantly enhance *RASSF1A* mRNA level compared to control group [Fig 11c]. This effect was not observed in free **L** treated cells, and the mRNA expression level was almost similar to that of control (Fig 11c).

3.11 Effect of free **L**, **1** and **2** on transforming growth factor- β (*TGF- β*)

Transforming growth factor-beta (*TGF- β*) is a multifunctional cytokine involved in the regulation of growth and differentiation of both normal and transformed cells. Therefore, we have investigated how these compounds effect the mRNA expression in hepatocellular carcinoma cell line. We found that all of our synthetic compounds insignificantly enhanced the mRNA expression of *TGF- β* (Fig 11d).

The ligand, **L** and its complexes **1** and **2** are tested for *in vitro* antitumor and anti-proliferative activity and expression of different genes involved in cancer. On the basis of our experimental results, complexes **1** and **2** showed a strong dose dependent growth inhibition of Huh7 cells compared to DMSO (control) treated cells. The free **L** exhibits least inhibitory effect compared to complexes **1** and **2**. The anti-proliferative effect of complexes **1** and **2** corroborate earlier

findings of palladium complexes derivatives that demonstrate a strong dose dependent growth inhibition [37, 38]. To determine whether these compounds effect key players in cancer, we measured the level of expression of Wnt-1, uPA, RASSF1 and TGF- β by real time PCR. In mammals, Wnt signaling is complex and regulates diverse functions including initiation and progression of cancer [39-42]. Therefore, we have tested the effect of our synthetic compounds on the mRNA expression of Wnt-1. Complexes **1** and **2** demonstrated significant inhibition of Wnt-1 expression compared to DMSO treated control. The free **L** treated cells showed decrease Wnt-1 mRNA expression but not significant like that of complexes **1** and **2**. These findings establish that the Pd(II) complexes have anti-proliferative and anticancer effects compared to parent ligand. Another important gene (uPA) analyzed in our study involves in metastatic cascade and implicate the degradation of the extracellular matrix and subsequent invasion by cancer cells [43-45]. Due the importance of this gene in metastasis, we analyzed its mRNA expression in the presence of the synthetic compounds. Surprisingly, none of the compounds suppress or activate the expression of uPA mRNA in Huh7 cell line. In most of the cancers, uPA is epigenetically regulated, as the promoter region of this gene hypomethylated [46]. The level of uPA mRNA expression is regulated by the methylation pattern (epigenome), it may a reason by these compounds had no effect on the expression of mRNA.

The Ras-association domain family 1A (RASSF1A) gene is a new candidate tumor suppressor gene (TSG) and has been reported to play an important role in the malignant progression of many tumors [47-49]. Due to its role in development of HCC, we have tested the expression of this gene in presence of our compounds. The finding was remarkable and showed enhanced RASSF1A expression in presence of complexes **1** and **2**, although free **L** expression was similar to the control group. We speculate that complexes **1** and **2** may involve in genetic alternations

[View Online](#)

and hence gain in RASSF1A expression. How these compounds alter the genetic structure needs to be analyzed in detail. Transforming growth factor- β (TGF- β) is a pleiotropic cytokine that regulates cell proliferation, angiogenesis, metastasis, and immune suppression [50, 51]. TGF- β has biphasic effect in tumor growth; carcinogenesis and early tumor growth are suppressed by TGF- β whereas this growth factor apparently accelerates tumor progression in more advanced aggressive tumors [49, 50]. Therefore, the effect of these compounds on the mRNA expression has been investigated. There was insignificant increase in the level of mRNA expression compared to control when Huh7 cells were treated with free **L** and complexes **1** and **2**.

4. Conclusion:

A series of novel mononuclear Pd(II) complexes derived from salen ligand has been synthesized and characterized by elemental analyses, and various spectroscopic studies. UV/Vis data reveal a square planar geometry around Pd(II) ion. The structure of ligand has been confirmed by single crystal XRD. The ligand and its complexes have been tested against human hepatoma cancer cell line and results suggest that Pd(II) complexes have significant anti-proliferative effects.

5. Supplementary material available:

CCDC876116 contains the supplementary crystallographic data for this paper. This data can be obtained free of charge from the Cambridge Crystallographic Data Centre via www.ccdc.cam.ac.uk/data_request/cif.

6. Acknowledgements:

This work is supported by Research Centre, College of Science, King Saud University, Riyadh KSA

7. References:

1. N.J. Wheate, S. Walker, G.E. Craig, R. Oun, Dalton Trans. 39 (2010) 8113–8127.
2. A.G. Quiroga, F.J. Ramos-Lima, A. Alvarez-Valdés, M. Font-Bardía, A. Bergamo, G. Sava C. Navarro-Ranninger, Polyhedron 30 (2011) 1646–1650.
3. S.J. Lippard, P. Pil, Encyclopedia of cancer, cis-platin and related drugs. San Diego, California: Academic Press, (1997) 392-410
4. F.J. Ramos-Lima, A.G. Quiroga, Jose M. Perez, Carmen Navarro-Ranninger, Polyhedron 22 (2003) 3379–3381
5. B. Lippert (Ed.), Cisplatin, 2006.
6. S. van Zutphen, J. Reedjik, Coord. Chem. Rev. 249 (2005) 2845–2853.
7. M.J. Clarke, F. Zhu, D.R. Frasca, Chem. Rev., 99 (1999) 2511
8. T. Schilling, B.K. Keppler, M.E. Heim, Invest, New Drugs, 13 (1996) 327
9. A.S. Abu-Surrah, M. Kettunen, Curr. Med. Chem. 13 (2006) 1337–1357.
10. G. Zhao, H. Lin, Curr. Med. Chem. Anticancer Agents 5 (2005) 137–147.
11. D.Kovala-Demertzi, A. Bocarelli, M.A. Demertzis, M. Coluccia, Chemotherapy 53 (2007) 148–152
12. N.J. Wheate, S. Walker, G.E. Craig, R. Oun, Dalton Trans. 39 (2010) 8113–8127.
13. E.C. Niederhoffer, J.H. Timmons, A.E. Martell, Chem. Rev. 84 (1984) 137
14. K. Srinivasan, P. Michaud, J.K. Kochi, J. Am. Chem. Soc. 108 (1986) 2309
15. W. Zhang, J.L. Loebach, S.R. Wilson, E.N. Jacobsen, J. Am. Chem. Soc., 112 (1990) 2801.
16. J. Tisato, F. Refosco, F. Bandoli, Coord. Chem. Rev. 135 (1994) 325.

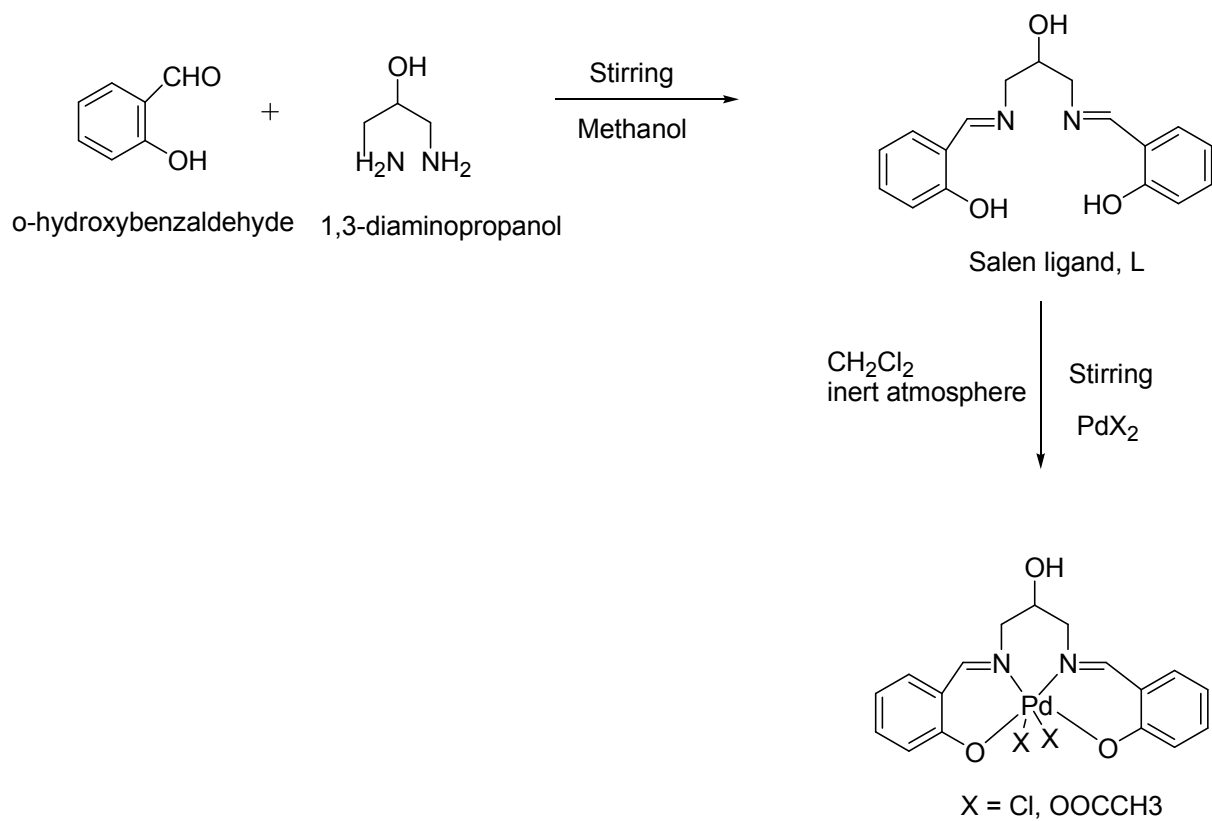
[View Online](#)

17. J. Fonseca, J. Martinez, Luís C.-Silva, A. L. Magalhães, M. T. Duarte, C. Freire, *Inorg. Chimica Acta*, 363 (2010) 4096-4107
18. X-RED. Version 1.18. STOE & Cie GmbH, Darmstadt, Germany (1999).
19. G.M. Sheldrick, A short history of SHELX, *Acta Crystallogr.* **A64** (2008) 112-122.
20. A.M. Pyle, J.P. Rehmman, R. Meshoyrer, C.V. Kumar, N.J. Turro, J.K. Barton, *J. Am. Chem. Soc.* 111 (1989) 3051–3058.
21. G.R. Desiraju, T. Steiner, *The Weak Hydrogen Bond in Structural Chemistry and Biology*, Oxford University Press, Oxford, 1999.
22. L.J. Baucher, *J. Inorg. Nucl. Chem.* 36 (1974) 531-536.
23. J. Uttamachandani, R.N. Kapoor, *Trans. Met. Chem.* 3 (1978) 79-81.
24. N. Dharmaraj, P. Viswanathamurthi, K. Natarajan, *Trans. Met. Chem.* 26 (2001) 105-109.
25. K. I. Goldberg, J. V.-Martinez, G.E.-Perez, L.J. Ackerman, D.X. West, *Polyhedron*, 18, 1999, 1177-1182
26. L.D. Popov, Y.P. Tupolova, V.V. Lukov, I.N. Shcherbakov, A.S. Burlov, S.I. Levchenkov, V.A. Kogan, K.A. Lyssenko, E.V. Ivannikova, *Inorganica Chimica Acta* 362 (2009) 1673–1680.
27. K. Nakamoto, *Infrared and Raman Spectra of Inorganic and Coordination Compounds* (Wiley, New York, 1986; Mir, Moscow 1991).
28. A.B.P. Lever, *Inorganic Electronic Spectroscopy*, second ed., Elsevier, New York, 1984.
29. M. Ulusoy, O. Birel, O. Sahin, O. Buyukgungor, B. Cetinkya, *Polyhedron* (2012) In press

30. H.H. Jaffe, M. Orchin, Theory and Applications of Ultraviolet Spectroscopy, J. Wiley, New York, 1962.
31. E.C. Long, J.K. Barton, *Acc. Chem. Res.* 23 (1990) 271.
32. R. Sujata, S. Rona, S. Munna, *J. Inorg. Biochem.* 100 (2006) 1320.
33. C. Liu, J. Zhou, *J. Inorg. Biochem.* 71 (1998) 1–6.
34. F. Leng, D. Graves, J.B. Chaires, *Biochim. Biophys. Acta* 1442 (1998) 71–81.
35. J. Liu, T. Zhang, T. Lu, L. Qu, H. Zhou, Q. Zhang, L. Ji, *J. Inorg. Biochem.* 91 (2002) 269–276
36. S. Yellappa, J. Seetharamappa, L.M. Rogers, R. Chitta, R.P. Singhal, F. D'Souza, *Bioconjugate Chem.*, 17 (2006) 1418-1425.
37. L. Giovagnini, L. Ronconi, D. Aldinucci, D. Lorenzon, S. Sitran, D. Fregona, *J Med Chem.* 48 (2005) 1588 -1595.
38. H. Cheng, F. Huq, P. Beale, K. Fisher, *Eur J Med Chem.* 41(2006) 896-903.
39. W. Wei, M.S. Chua, S. Grepper, *Mol Cancer.* 8 (2009) 76
40. Y. Takigawa, A.M. Brown, *Curr Drug Targets.* 9 (2008) 1013-1024.
41. S.B. Nambotin, J.R. Wands, M. Kim, *Anticancer Agents Med Chem.* 11(2011) 549-559.
42. H.C. Lee, M. Kim, J.R. Wands, *Front Biosci.* 11 (2006) 1901-1915
43. P.A. Andreasen , L. Kjoller, L. Christensen, M.J. Duffy, *Int J Cancer.* 72 (1997) 1-22
44. S.A. Rabbani, *In Vivo.* 12 (1998) 135-142.
45. S.A. Rabbani, A.P. Manzar, *SurgOncol Clin N Am.* 10 (2001) 393-415
46. N. Shukeir, P. Pakneshan, G. Chen, M. Szyf, S.A. Rabbani, *Cancer Res.* 66 (2006) 9202-9210.

[View Online](#)

47. R. Dammann, C. Li, J.H. Yoon, P.L. Chin, S. Bates, G.P. Pfeifer, *Nat Genet.* 25 (2000) 315–19.
48. K. Dreijerink, E. Braga, I. Kuzmin, *Proc Natl Acad Sci. USA* 98 (2001) 7504–7509.
49. L. Shivakumar, J. Minn, T. Sakamaki, R. Pestell, M.A. White, *Mol Cell Biol.* 22 (2002) 4309–4318.
50. A. Nawshad, D. Lagamba, A. Polad, E.D. Hay, *Cells Tissues Organs* 179 (2005) 11–23
51. R.L. Elliott, G.C. Blobe, *J Clin Oncol* 23 (2005) 2078–2093.



Scheme: Schematic representation of synthesis of salen ligand and its Pd(II) complexes

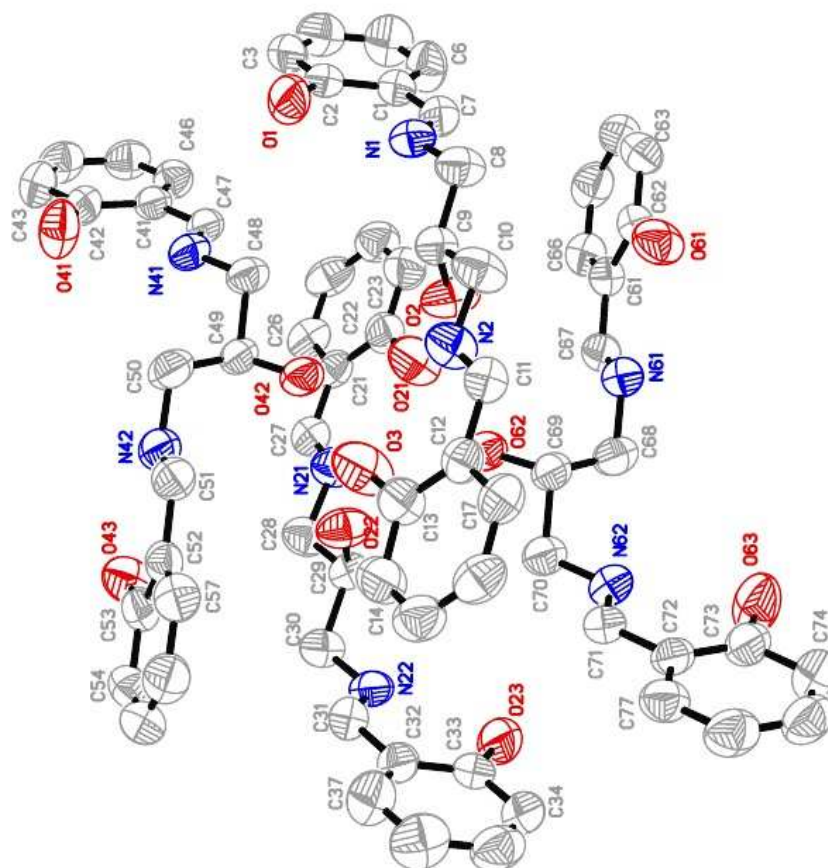


Fig 1: Ortep diagram of free Ligand, L plotted with 50% probability of displacement ellipsoids. The part of atoms labels and hydrogen atoms were omitted for clarity.

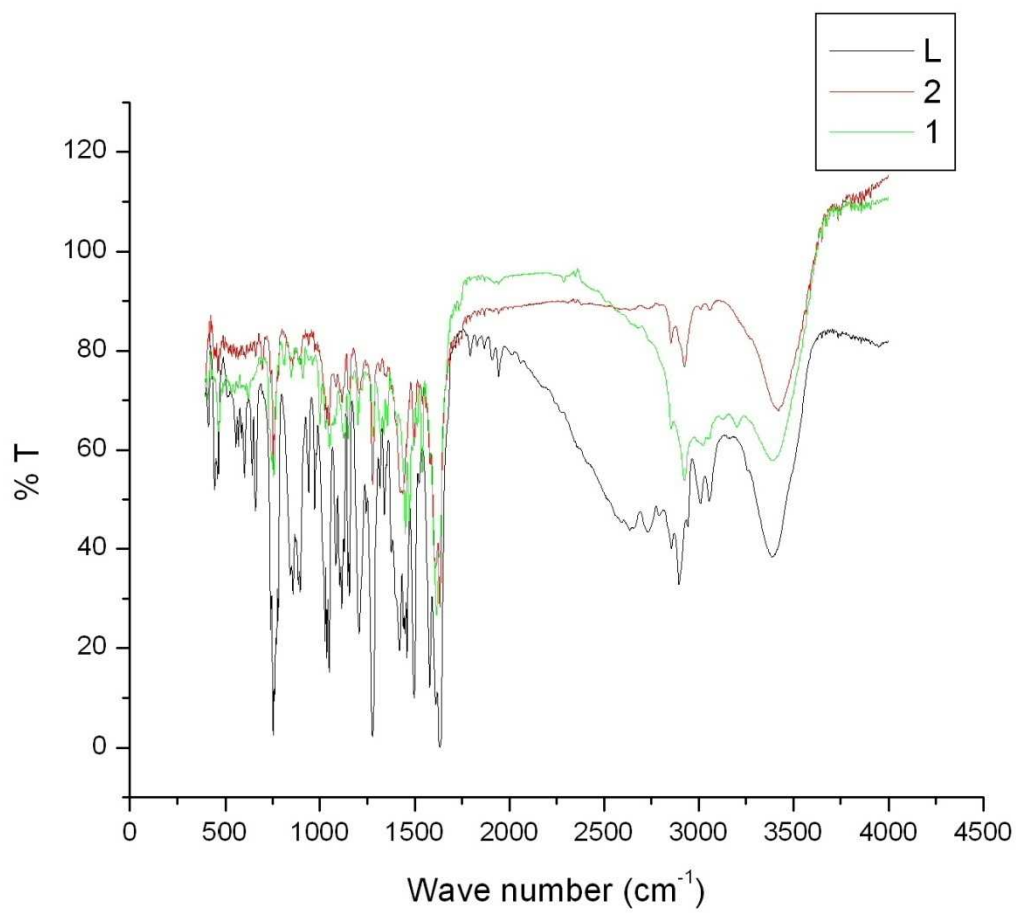


Fig 2: IR Spectra of ligand, L, Complex 1 and 2

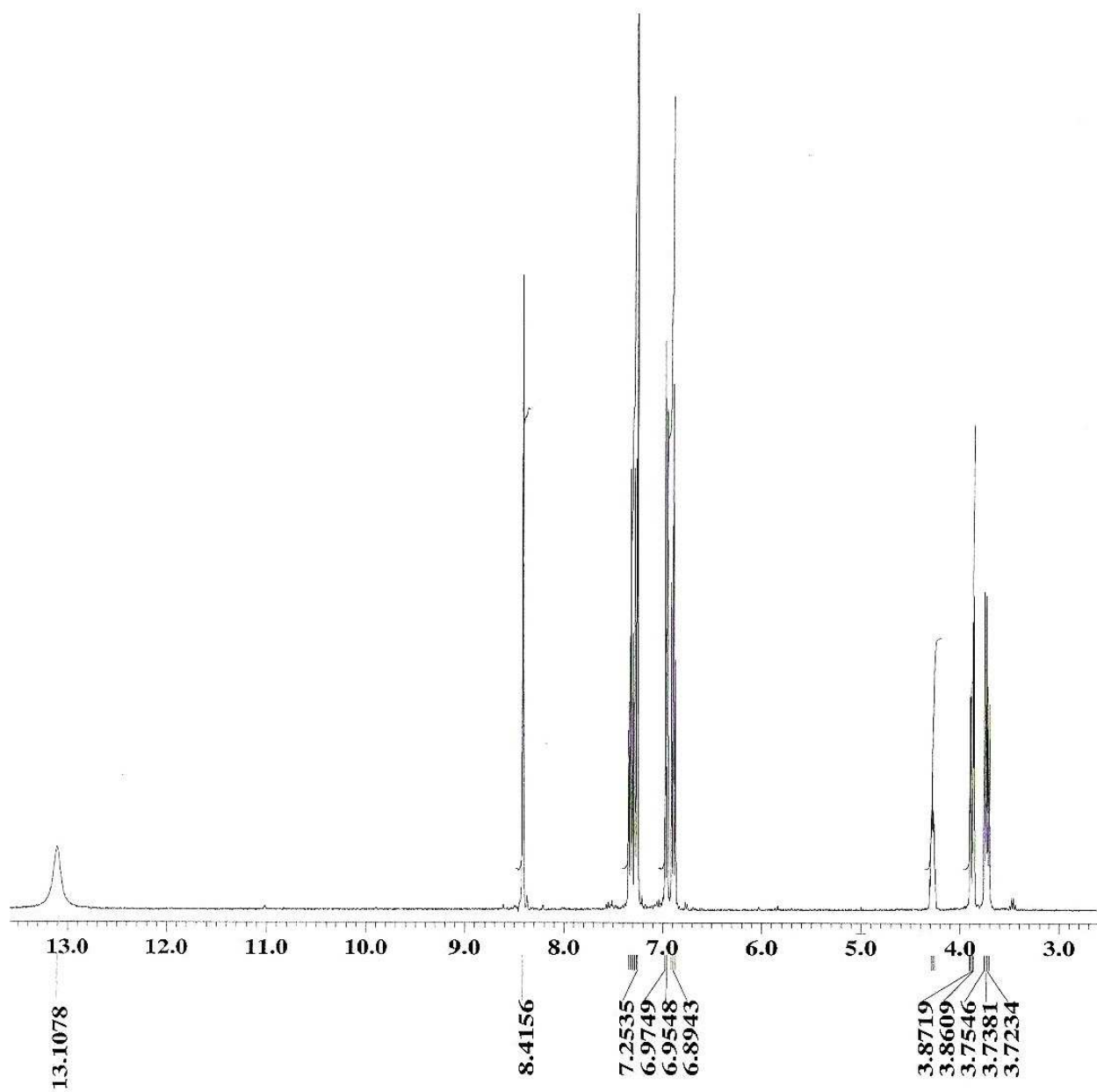


Fig 3: ¹H NMR Spectrum of Complex 1

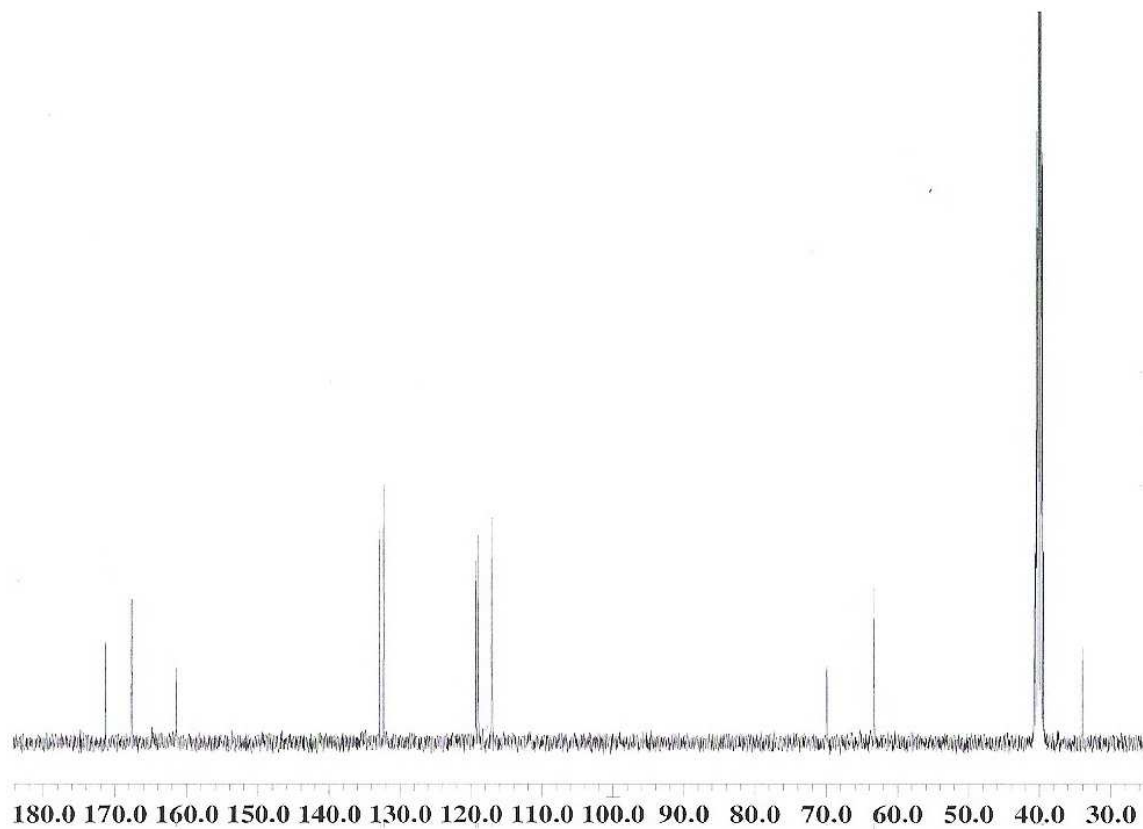


Fig 4: ^{13}C NMR spectrum of Complex 2

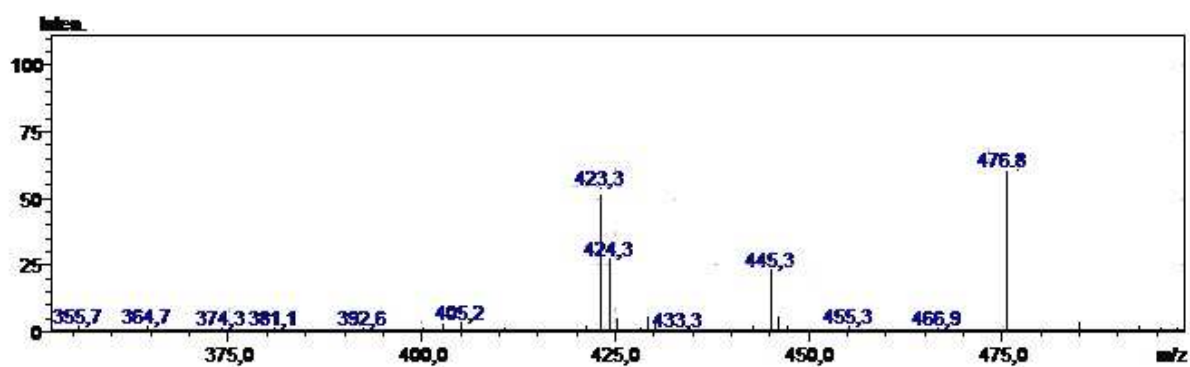


Fig 5: ESI-MS Spectrum of Complex 1

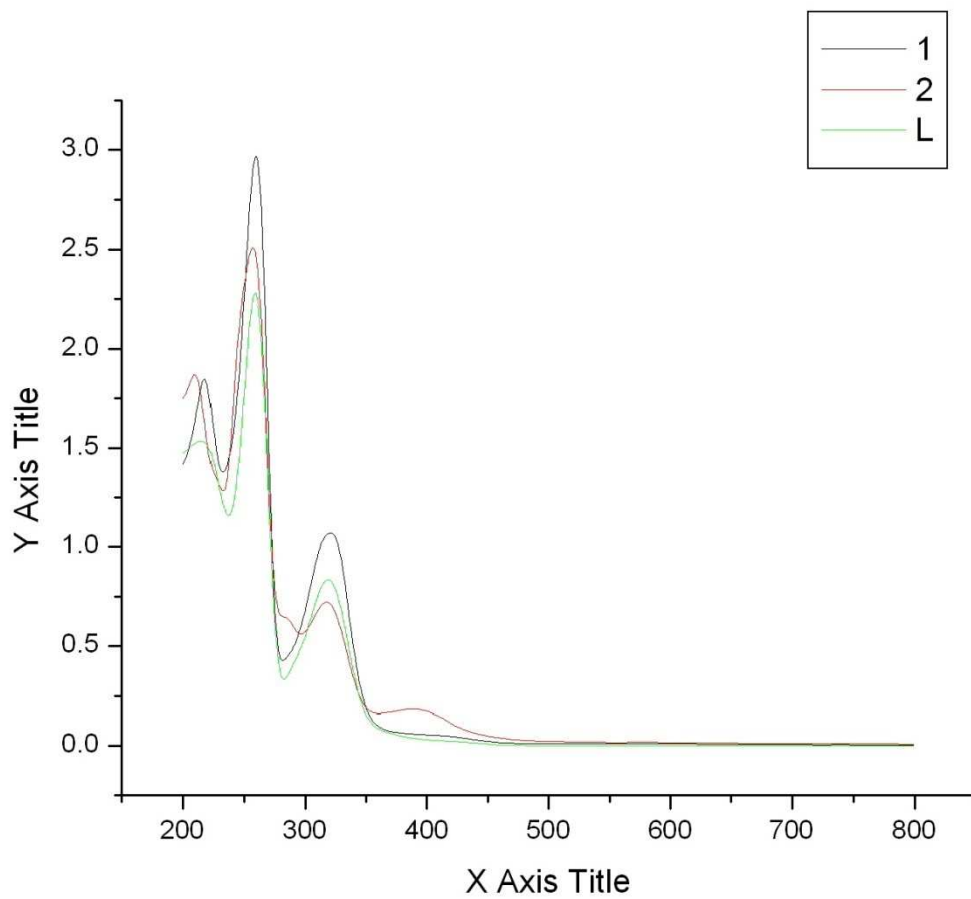


Fig 6: UV-Vis spectra of ligand, L and Complexes 1 and 2

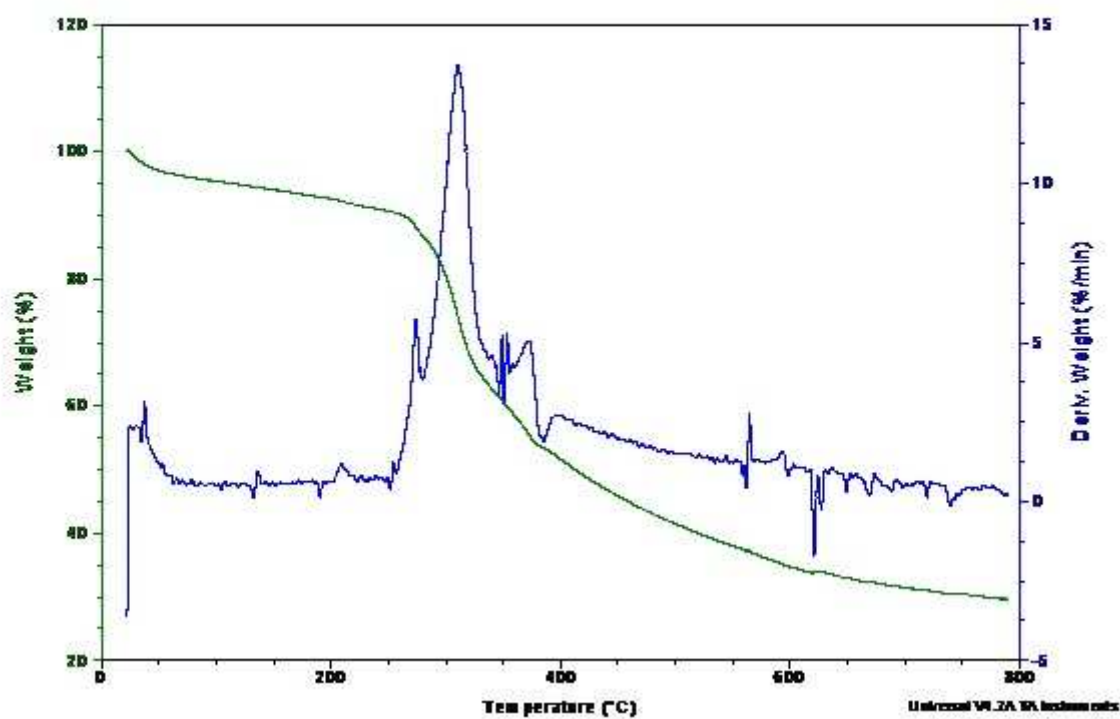


Fig 7: TGA/DTA curve of complex 1

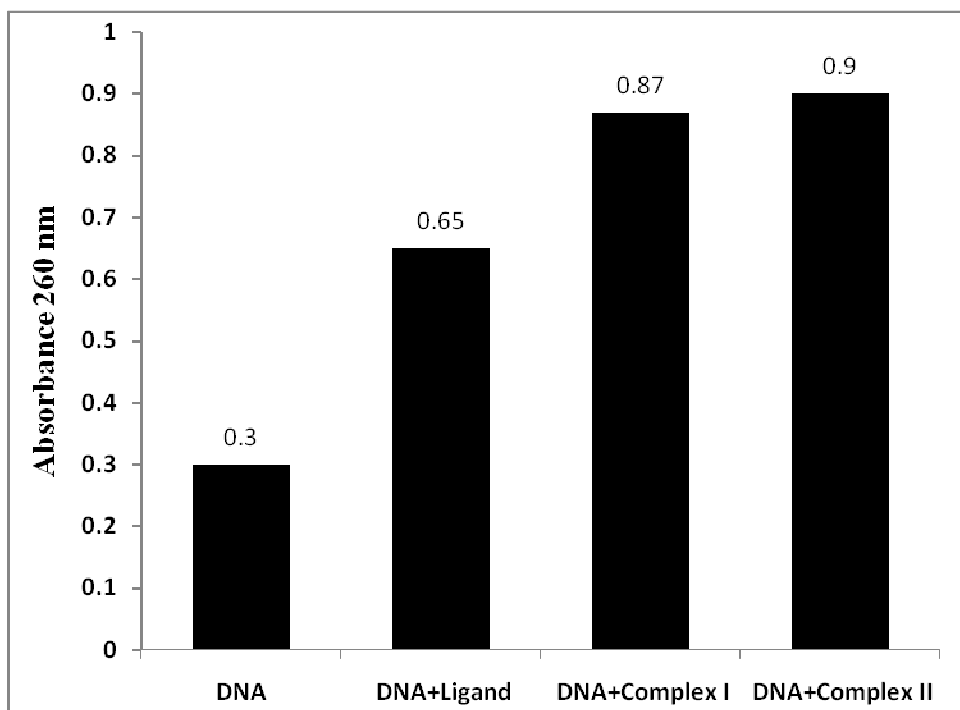


Fig 8: Absorbance spectroscopy of DNA at 260 nm with Ligands and its complexes: DNA concentration was 0.1 mM and the concentration of ligand and its both complexes were 50 μ M.

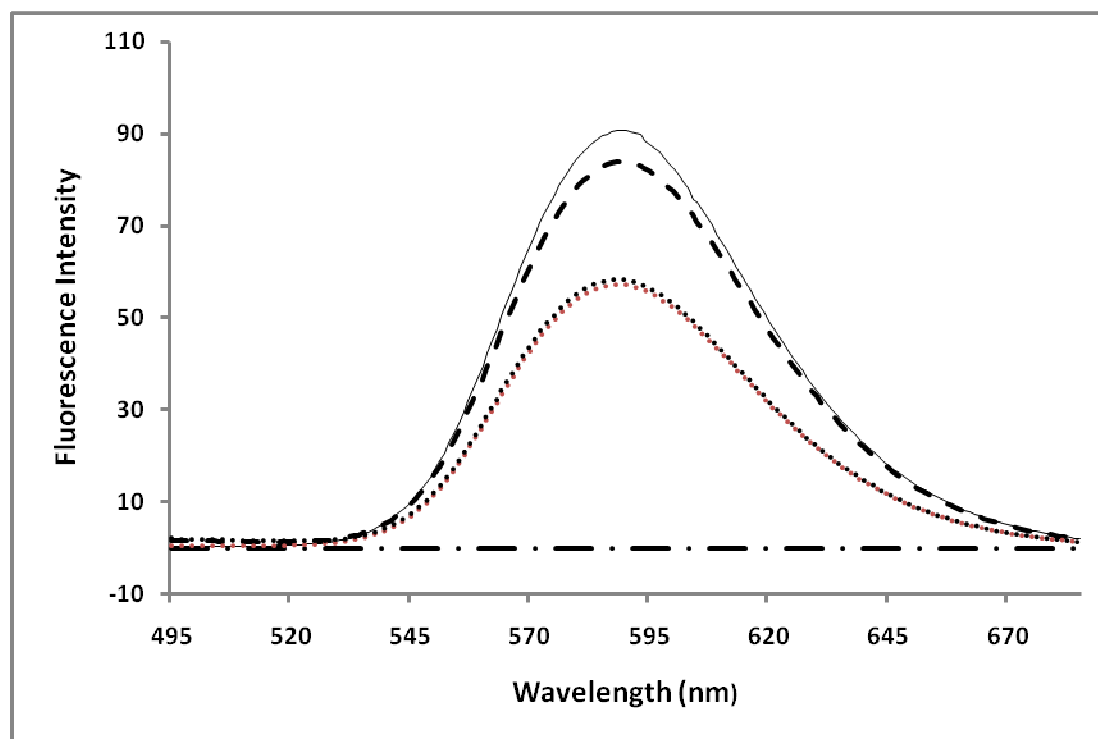


Fig 9: Fluorescence emission spectra of ethidium bromide (EB) bound to DNA in the absence and presence of ligand and complex. EB alone (- · -); EB + DNA (—); EB + DNA + ligand (— —); EB + DNA + complex 1 (— · —), EB + DNA + complex 2 (· · ·).

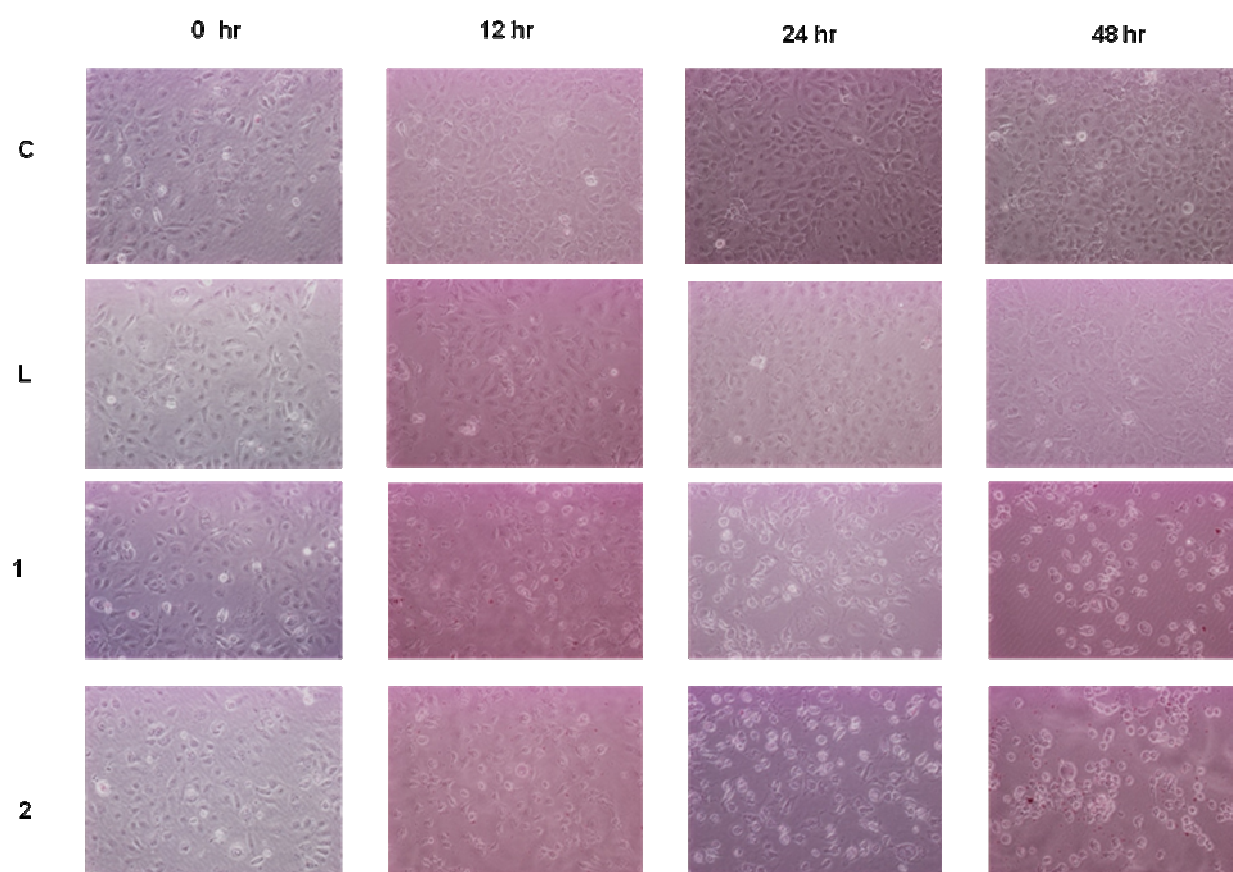


Fig 10 (a):

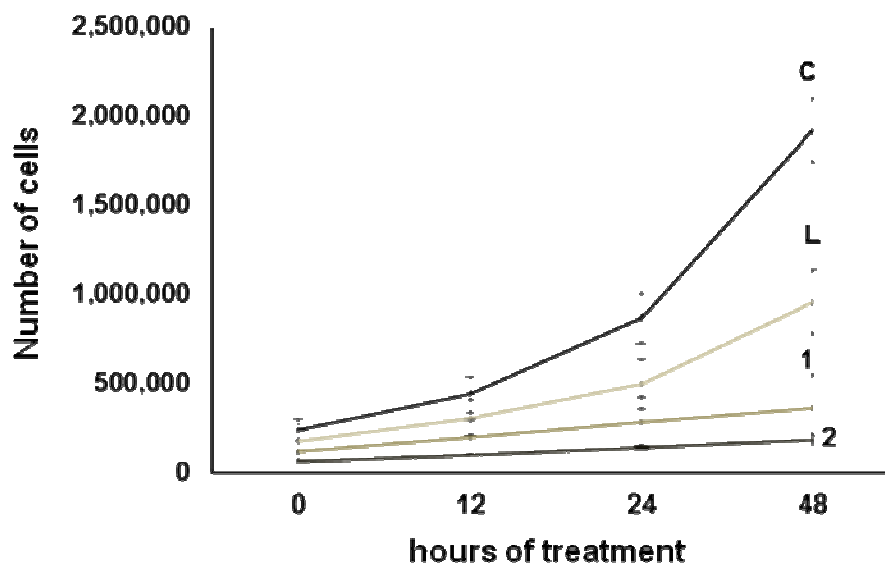


Fig 10 (b):

Fig 10 : Effect of Ligand, L alone, Complexes 1 and 2 on the proliferation of Huh7 cells. Huh7 cells were seeded at the same density a day before treatment. Next day the cells were subjected treatment with an optimized concentration of L alone, complexes 1 and 2 and vehicle control alone (DMSO) in a six well plate. The anti-proliferative effect of these compounds was measured microscopically at different time intervals and also by growth curve analysis. At each time point (12 hrs, 24 hrs & 48 hrs), cells were trypsinized and counted as described in Materials and Methods section. All data presented are expressed as mean \pm SEM of triplicate wells for each time point. Significant difference from the control is represented by an asterisk ($P < 0.05$).

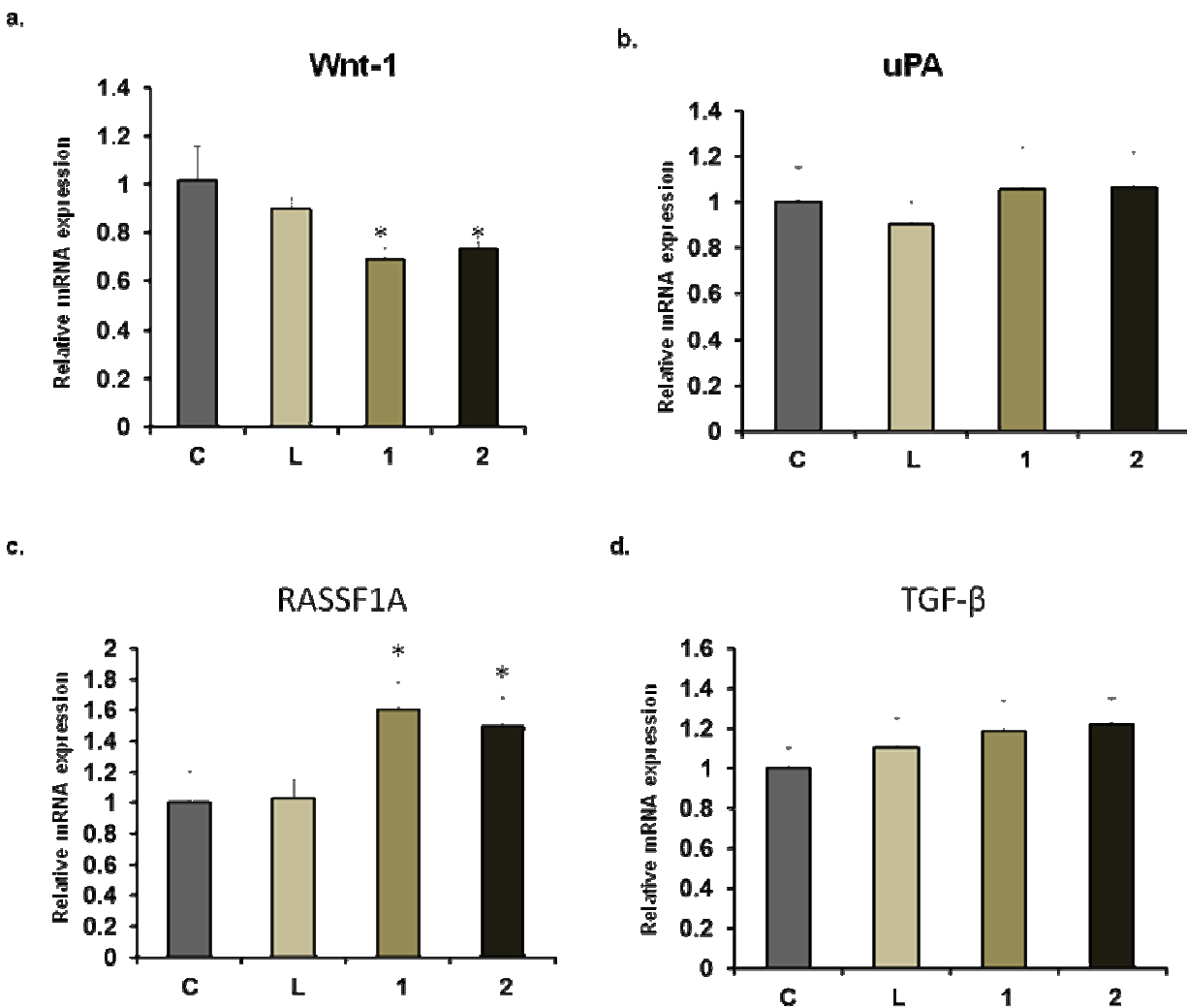


Fig 11: Effect of Ligand, L alone and Complexes 1 and 2 on the expression of tumor promoting and suppressor genes. Huh7 cells were treated Ligand, L alone, Complexes 1 and 2 and at the end of experiment, total cellular RNA was isolated with Trizol. RNA from control and treatment groups were analyzed for the expression of genes 10a) Wnt, 10b) uPA, 10c) RASSF1A and 10d) TGF- β by real time PCR. Changes in the mRNA expression of the respective genes were determined as relative mRNA expression against internal control GAPDH. The experiment was repeated thrice and significant difference from the control is represented by an asterisk ($P < 0.05$).

[View Online](#)Table 1. Crystal and structure refinement data of compound **1**

Compound	1
Empirical formula	C ₁₇ H ₁₈ N ₂ O ₃
Formula weight	298.33
Crystal system, space group	monoclinic, <i>C c</i> (No. 9)
Unit cell dimensions [Å, °]	<i>a</i> = 35.6816(19) <i>b</i> = 11.2773(4) <i>c</i> = 16.3321(9) β = 109.142(4)
Volume [Å ³]	6208.5(5)
Z, Calculated density [Mg/m ³]	16, 1.277
Absorption coefficient [mm ⁻¹]	0.721
<i>F</i> (000)	2528
Crystal size [mm]	0.066, 0.061, 0.060
θ range for data collection [°]	2.62 to 68.04
Index ranges	-42 ≤ <i>h</i> ≤ 42, -10 ≤ <i>k</i> ≤ 13, -19 ≤ <i>l</i> ≤ 19
Reflections collected / unique	35541 / 10801 [<i>R</i> _(int) = 0.0256]
Completeness [%]	99.3 (to θ = 67°)
Min. and max. transmission	0.948 and 0.963
Data / restraints / parameters	10801 / 2 ^s / 806
Goodness-of-fit on <i>F</i> ²	1.021
Final <i>R</i> indices [<i>I</i> > 2σ(<i>I</i>)]	<i>R</i> 1 = 0.0369, <i>wR</i> 2 = 0.1067
<i>R</i> indices (all data)	<i>R</i> 1 = 0.0383, <i>wR</i> 2 = 0.1092
Largest diff. peak and hole [e•Å ⁻³]	0.227, -0.172

^sFloating origin restraints

Table 2. Selected structural data of compound **1** [\AA , $^\circ$].

C2—O1	1.332(2)	C22—O21	1.325(2)	C42—O41	1.343(3)	C62—O61	1.341(2)
C7—N1	1.266(2)	C27—N21	1.257(2)	C47—N41	1.276(2)	C67—N61	1.269(2)
N1—C8	1.447(2)	N21—C28	1.465(2)	N41—C48	1.456(2)	N61—C68	1.455(2)
C9—O2	1.409(2)	C29—O22	1.405(2)	C49—O42	1.411(2)	C69—O62	1.418(2)
C10—N2	1.459(2)	C30—N22	1.454(2)	C50—N42	1.453(2)	C70—N62	1.448(2)
N2—C11	1.265(2)	N22—C31	1.260(2)	C51—N42	1.260(3)	N62—C71	1.269(2)
C13—O3	1.340(2)	C33—O23	1.345(3)	C53—O43	1.344(2)	C73—O63	1.348(3)
C7—N1—C8	119.8(2)	C27—N21—C28	119.7(2)	C47—N41—C48	117.8(2)	C67—N61—C68	119.8(2)
C11—N2—C10	119.1(2)	C31—N22—C30	119.6(2)	C51—N42—C50	119.6(2)	C71—N62—C70	119.0(2)
C2—C1—C7—N1	-1.8(3)	C22—C21—C27—N21	-0.6(3)	C42—C41—C47—N41	1.9(3)	C62—C61—C67—N61	-0.5(3)
C1—C7—N1—C8	178.3(2)	C21—C27—N21—C28	177.2(2)	C41—C47—N41—C48	179.3(2)	C61—C67—N61—C68	179.7(2)
C7—N1—C8—C9	128.3(2)	C27—N21—C28—C29	171.9(2)	C47—N41—C48—C49	-124.7(2)	C67—N61—C68—C69	-103.2(2)
N1—C8—C9—C10	169.4(2)	N21—C28—C29—C30	-175.8(2)	N41—C48—C49—C50	-63.3(2)	N61—C68—C69—C70	-176.7(2)
C8—C9—C10—N2	-174.7(2)	C28—C29—C30—N22	171.5(2)	C48—C49—C50—N42	175.9(2)	C68—C69—C70—N62	59.9(2)
C9—C10—N2—C11	-175.6(2)	C29—C30—N22—C31	123.4(2)	C49—C50—N42—C51	103.8(2)	C69—C70—N62—C71	127.4(2)
C10—N2—C11—C12	177.9(2)	C30—N22—C31—C32	-179.5(2)	C50—N42—C51—C52	-178.9(2)	C70—N62—C71—C72	-178.2(2)
N2—C11—C12—C13	-2.7(3)	N22—C31—C32—C33	0.4(3)	N42—C51—C52—C53	1.4(3)	N62—C71—C72—C73	-0.3(3)

[View Online](#)Table 3. Hydrogen bonds geometry of compound **1** [\AA , $^\circ$].

D—H...A	d(D-H)	d(H...A)	d(D...A)	\angle (DHA)
O1—H1—N1	0.82	1.89	2.601(2)	145.1
O2—H2—O21 ⁱ	0.82	2.39	2.921(2)	123.7
O3—H3A—N2	0.82	1.89	2.610(2)	146.9
O21—H21—N21	0.82	1.85	2.578(2)	148.0
O22—H22—O62 ⁱⁱ	0.89	2.20	2.976(2)	145.4
O23—H23A—N22	0.82	1.85	2.577(2)	147.7
O41—H41—N41	0.82	1.89	2.598(2)	144.5
O42—H42—O22	0.82	2.04	2.851(2)	171.3
O43—H43A—N42	0.82	1.86	2.587(2)	147.5
O61—H61—N61	0.82	1.86	2.587(2)	146.3
O62—H62—O2 ⁱⁱⁱ	0.82	2.03	2.837(2)	166.5
O63—H63A—N62	0.82	1.87	2.599(2)	147.6
C25—H25—O1 ^{iv}	0.93	2.57	3.215(3)	126.4
C50—H50B—N41	0.97	2.62	2.978(3)	102.3
C68—H68A—N62	0.97	2.60	2.954(3)	101.7

Symmetry transformations used to generate equivalent atoms: (i) $x, -y+1, z+1/2$; (ii) $x-1/2, y-1/2, z$; (iii) $x+1/2, -y+3/2, z-1/2$; (iv) $x, y, z-1$

Table 4: Primer sequence and annealing temperatures used for real time PCR

Primer Name	Primer sequence	Annealing (°C)
Wnt-1	ACTCTCAGGACATGCTGGCT ACGAGGTCATTTTCGTTGG	59
RASSF1A	ACCTCTGTGGCGACTTCATCT AGGTGAACTTGCAATGCGC	60
uPA	TTGCTCACCACAACGACATT GGCAGGCAGATGGTCTGTAT	56
TGF- β	CAAGGACCTCGGCTGGAA CCGGGTTATGCTGGTTGTACA	58
GAPDH	CGACCACTTGTCAAGCTCA AGGGGTCTACATGGCAACTG	55-60

[View Online](#)

Two novel Pd(II) complexes has been derived from o-hydroxybenzaldehyde and 1,3-diaminopropanol and characterized on the basis of various physic-chemical studies. The free salen ligand and its Pd(II) complexes have been tested against human hepatoma cancer cell line (Huh7) and results manifested excellent anti-proliferative effects of Pd(II) complexes.

